0026-895X/10/7703-459–468$20.00
MOLECULAR PHARMACOLOGY
Vol. 77, No. 3
58768/3564947
Mol Pharmacol 77:459–468, 2010
Printed in U.S.A.

Context-Dependent Pharmacology Exhibited by Negative Allosteric Modulators of Metabotropic Glutamate Receptor 7[S]

Colleen M. Niswender, Kari A. Johnson, Nicole R. Miller, Jennifer E. Ayala, Qingwei Luo, Richard Williams, Samir Saleh, Darren Orton, C. David Weaver, and P. Jeffrey Conn

Department of Pharmacology and Vanderbilt Program in Drug Discovery (C.M.N., K.A.J., N.R.M., J.E.A., Q.L., R.W., C.D.W., P.J.C.), Vanderbilt Institute of Chemical Biology (S.S., D.O., C.D.W.), Department of Chemistry (D.O.), Vanderbilt University, Nashville, Tennessee

Received June 22, 2009; accepted December 18, 2009

ABSTRACT

Phenotypic studies of mice lacking metabotropic glutamate receptor subtype 7 (mGluR7) suggest that antagonists of this receptor may be promising for the treatment of central nervous system disorders such as anxiety and depression. Suzuki et al. (*J Pharmacol Exp Ther* **323:**147–156, 2007) recently reported the in vitro characterization of a novel mGluR7 antagonist called 6-(4-methoxyphenyl)-5-methyl-3-(4-pyridinyl)-isoxazolo[4,5-c]pyridin-4(5H)-one (MMPIP), which noncompetitively inhibited the activity of orthosteric and allosteric agonists at mGluR7. We describe that MMPIP acts as a noncompetitive antagonist in calcium mobilization assays in cells coexpressing mGluR7 and the promiscuous G protein $G\alpha_{15}$. Assessment of the activity of a small library of MMPIP-derived compounds using this assay reveals that, despite similar potencies, compounds exhibit differences in negative cooperativity for agonist-mediated calcium mobilization. Examination of the inhibitory activity of MMPIP and analogs using endogenous $G_{i/o}$-coupled assay readouts indicates that the pharmacology of these ligands seems to be context-dependent, and MMPIP exhibits differences in negative cooperativity in certain cellular backgrounds. Electrophysiological studies reveal that, in contrast to the orthosteric antagonist (2*S*)-2-amino-2-[(1*S*,2*S*)-2-carboxycyclcoprop-1-yl]-3-(xanth-9-yl) propanoic acid (LY341495), MMPIP is unable to block agonist-mediated responses at the Schaffer collateral-CA1 synapse, a location at which neurotransmission has been shown to be modulated by mGluR7 activity. Thus, MMPIP and related compounds differentially inhibit coupling of mGluR7 in different cellular backgrounds and may not antagonize the coupling of this receptor to native $G_{i/o}$ signaling pathways in all cellular contexts. The pharmacology of this compound represents a striking example of the potential for context-dependent blockade of receptor responses by negative allosteric modulators.

The G protein-coupled receptors (GPCRs) play critical roles in regulating a broad range of signaling pathways within virtually every organ system (George et al., 2002) and are the targets of intense discovery efforts for new drug candidates. Despite this concentrated focus, selective ligands do not exist for the majority of these receptors (Howard et al., 2001). Many GPCRs interact with natural ligands based on complex or highly restricted chemical scaffolds (for example, amino acids, peptides, lipids, etc.) that are not well suited to optimization of selective small-molecule reagents. In addition, high conservation of the orthosteric sites of GPCR subfamilies presents challenges in developing high selectivity for a given receptor subtype. For these reasons, increasing interest has been placed on identifying compounds that interact with GPCRs at allosteric, rather than orthosteric, binding

This work was supported by the National Institutes of Health National Institute of Neurological Disorders and Stroke [Grants NS053536, NS031373, NS048334] and the Michael J. Fox Foundation.

Portions of this work were presented at the 2007 Society for Neuroscience Meeting (2007 Nov 3–7; San Diego, CA); the 45th Annual Meeting of the American College of Neuropsychopharmacology (2006 Dec 3–7; Hollywood, FL); and the 6th International Meeting on Metabotropic Glutamate Receptors (2008 Sept 14–19; Taormina, Sicily, Italy).

Article, publication date, and citation information can be found at http://molpharm.aspetjournals.org.

doi:10.1124/mol.109.058768.

[S] The online version of this article (available at http://molpharm.aspetjournals.org) contains supplemental material.

ABBREVIATIONS: GPCR, G protein-coupled receptor; GIRK, G protein-regulated inwardly rectifying potassium channel; mGluR, metabotropic glutamate receptor; HEK, human embryonic kidney; DMSO, dimethyl sulfoxide; L-AP4, L-(+)-amino-4-phosphonobutyric acid; LY341495, (2*S*)-2-amino-2-[(1*S*,2*S*)-2-carboxyclycloprop-1-yl]-3-(xanth-9-yl) propanoic acid; MMPIP, 6-(4-methoxyphenyl)-5-methyl-3-(4-pyridinyl)-isoxazolo[4,5-c]pyridin-4(5*H*)-one; AMN082, *N*,*N*′-dibenzhydrylethane-1,2-diamine dihydrochloride; PAM, positive allosteric modulator; NAM, negative allosteric modulator; CNS, central nervous system; DMEM, Dulbecco's modified Eagle's medium; ACSF, artificial cerebrospinal fluid; BHK, baby hamster kidney; fEPSP, field excitatory postsynaptic potential; PICK1, protein interacting with C kinase 1; SC-CA1, Schaffer collateral-CA1; VUSC001, 6-(4-methoxyphenyl)-5-methyl-3-phenylisoxazolo[4,5-*c*]pyrdin-4(5*H*)-one; VUSC027, 6-(3-methoxyphenyl)-5-methyl-3-phenylisoxazolo-[4,5-*c*]pyridine-4(5*H*)-one.

sites to modulate receptor function. Both positive allosteric modulators (PAMs) and negative allosteric modulators (NAMs) have been described for multiple GPCRs that possess high subtype selectivity and are suitable for the modulation of receptor function in both in vitro and in vivo settings (Gilchrist and Blackmer, 2007; Conn et al., 2009; Groebe, 2009).

Although allosteric modulators of GPCRs provide potential advantages over traditional orthosteric ligands, these compounds also introduce new layers of complexity into receptor pharmacology. In recent years, there has been a growing appreciation of the ability of a single GPCR to simultaneously regulate multiple signaling pathways (Kenakin, 2005). Furthermore, ligands can stabilize distinct conformational states of GPCRs, activating or inhibiting a discrete subset of the possible cellular behaviors linked to that receptor. The phenomenon by which different ligands can preferentially stabilize discrete receptor conformations and differentially affect various signaling pathways has been termed "functional selectivity" or "ligand-directed trafficking of receptor stimulus" (Leach et al., 2007; Urban et al., 2007). In addition to the ability of unique ligands to preferentially stabilize specific receptor confirmations to affect signaling, the context for receptor expression may also play a critical role in the pharmacology of individual ligands. Differences in the G protein complement or other receptor-interacting proteins within a cell, for example, may engender different receptor conformations or signaling (in the presence or absence of agonist), potentially altering ligand pharmacology.

Because allosteric modulators stabilize different conformational states of GPCRs, it is anticipated that these compounds could engender functionally selective or context-dependent effects in the actions of orthosteric ligands that cobind to the receptor. There are now examples of differential signaling effects induced by the actions of GPCR PAMs (Zhang et al., 2005), as well as examples of the "probe dependence" of allosteric modulators (i.e., that certain modulators will behave differently in the presence of distinct orthosteric ligands) (Kenakin, 2008). NAMs can also theoretically stabilize distinct receptor conformations, preventing orthosteric agonists from activating some but not all signaling pathways or exhibiting differential levels of negative cooperativity on agonist affinity or efficacy (Kenakin, 2005). Although functionally selective and context-dependent behavior of compounds introduces potential complexity into ligand development, it is anticipated that this phenomenon will provide exciting opportunities to tailor new drug therapy to specifically affect coupling of GPCRs to some signaling pathways but not others.

Suzuki et al. recently reported the discovery of the compound MMPIP as a highly selective NAM of the metabotropic glutamate receptor subtype 7 (mGluR7) that exhibits intrinsic inverse agonist activity (Suzuki et al., 2007; Nakamura et al., 2010). This compound represents a major breakthrough in that it is the first selective antagonist of mGluR7, a receptor that is believed to play critical roles in regulating excitatory synaptic transmission in many regions of the CNS (Pelkey et al., 2005; Ayala et al., 2008; de Rover et al., 2008). We synthesized MMPIP and multiple MMPIP analogs to develop a further understanding of the actions of this compound. Consistent with previous findings (Suzuki et al., 2007), we observed that MMPIP and related compounds blocked mGluR7-mediated increases in intracellular calcium mobilization via a promiscuous G protein. However, MMPIP and its analogs exhibited lower potencies and efficacies as antagonists of mGluR7 coupling to G protein-coupled inwardly rectifying potassium (GIRK) channels through endogenous cellular G proteins. Activity of MMPIP on the coupling of mGluR7 to inhibition of cAMP accumulation in this same cell line was complex; the compound seemed to inhibit constitutive activity of the receptor but did not block the cAMP inhibition response induced by an orthosteric agonist. MMPIP was further examined using a label-free technology to directly compare mGluR7 responses in distinct cell backgrounds. In these studies, it was clear that MMPIP exhibited different pharmacology depending on the cell background for expression. Finally, MMPIP did not block the effects of an mGluR7 agonist at a glutamatergic synapse in the hippocampus, in which a role for mGluR7 has been established previously (Ayala et al., 2008). Because regulation of transmission at excitatory synapses is believed to be a major role of mGluR7, these findings suggest that MMPIP may not block many of the predominant effects of mGluR7 in vivo. These results suggest that the actions of MMPIP and potentially other GPCR NAMs may be highly specific for modulating signaling pathways in different cellular contexts.

Materials and Methods

Cell Lines and Cell Culture. Baby hamster kidney (BHK) cells stably expressing rat mGluR7a were transfected with a pcDNA 3.1+ plasmid encoding $G\alpha_{15}$ (Conklin et al., 1993). Cells were grown in Dulbecco's modified Eagle's medium (DMEM) containing 10% fetal bovine serum, 20 mM HEPES, 2 mM L-glutamine, 100 mM penicillin/streptomycin, 1× nonessential amino acids, 1 μM methotrexate, and 400 μg/ml G418 (Mediatech, Inc., Herndon, VA) at 37°C in the presence of 5% CO_2. Rat mGluR7a/HEK/GIRK cells were grown in growth medium (45% DMEM, 45% Ham's F-12, 10% fetal bovine serum, 20 mM HEPES, 2 mM L-glutamine, 100 mM penicillin/streptomycin, nonessential amino acids, 700 μg/ml G418, and 0.6 μg/ml puromycin) at 37°C in the presence of 5% CO_2. For both cell lines, cells were plated for assays in assay medium (DMEM, 10% dialyzed fetal bovine serum, 20 mM HEPES, and 1 mM sodium pyruvate). All cell culture reagents were purchased from Invitrogen (Carlsbad, CA) unless otherwise noted.

Calcium Assays. One day before assay, cells were plated at 30,000 cells/well in a black-walled, clear-bottomed 384-well plate (Greiner Bio-One, Longwood, FL) in glutamine-free medium and subjected to heat shock at 42°C for 2.5 h. Cells were incubated at 37°C, 5% CO_2 overnight. The following day, cells were incubated for 1 h at room temperature with 20 μl of 3 μM Fluo-4/acetoxymethyl ester, prepared as a 2.3 mM stock in DMSO, mixed in a 1:1 ratio with 10% (w/v) Pluronic acid F-127 (Invitrogen), and diluted in calcium assay buffer (Hanks' balanced salt solution, 20 mM HEPES, and 2.5 mM probenecid). Dye was then replaced with 20 μl of calcium assay buffer. MMPIP-derived test compounds and the group III mGluR agonist L-AP4 were prepared at 2.5 or 5 times their final concentrations, respectively, in calcium assay buffer. After initial fluorescence readings in a Hamamatsu imaging-based plate reader (excitation, 470 ± 20 nm; emission, 540 ± 30 nm; FDSS6000; Hamamatsu Corporation, Bridgewater, NJ), 20 μl of test compound was added to cells, and fluorescence was measured every 24 s for 30 min. Vehicle or agonist (10 μl) was then added, and fluorescence was measured every second for 2 min. Raw data were exported to Excel (Microsoft, Redmond, CA), and the maximum fluorescence reading for each trace was measured. Concentration-response curves were integrated and fitted using a four-parameter logistic equation in Prism (GraphPad Software, Inc., San Diego, CA).

Thallium Flux Assays. Thallium flux assays for mGluRs 7, 4, and 8 were performed as described in Niswender et al., (2008) using the Hamamatsu FDSS6000. In brief, cells were plated at 15,000 cells/well on poly(D-lysine)-coated 384-well plates (Greiner Bio-One) in assay medium (Niswender et al., 2008), and the following day, the medium was replaced with 20 μl of either 1.7 μM betacellulin, acetoxymethyl ester, or 0.33 μM Fluo-Zn^{2+} (FluxOr; Invitrogen) [dyes were premixed 1:1 with 10% Pluronic acid 127 and then dissolved in assay buffer (Hanks' balanced salt solution and 20 mM HEPES assay buffer]. Cells were incubated with dye for 45 min, and the dye was removed and replaced with 20 μl of assay buffer. Baseline fluorescence readings were taken for 3 s, 20 μl of 2.5× antagonist was added, and fluorescence was measured every 2 s for 5 min. L-AP4 or glutamate (10 μl) was then added, and fluorescence was measured for an additional 2 min. Fluorescence traces were analyzed by calculating the slope of the change in fluorescence from 10 to 20 s after agonist/thallium addition. In full concentration-response curve experiments of MMPIP, nonspecific effects induced by MMPIP were apparent from parallel experiments with mGluR4, mGluR8, and M4 muscarinic receptor experiments (Fig. 3B) and are most likely due to nonspecific inhibition of the GIRK channel or another mechanism mediating background thallium flux in these cells. To correct for these apparent nonspecific effects, concentration-response data were expressed as the percentage of relative EC_{80} response for each cell line. mGluR7 data were then normalized to the responses obtained in M4-expressing cells by using the following formula: 100 − (%EC_{80} response obtained in M4-expressing cells minus the %EC_{80} response obtained in mGluR7-expressing cells). M4 was chosen because it is an unrelated and family A GPCR, but the data from Fig. 3B clearly indicate that mGluR4-, 8-, and M4-expressing cells showed almost identical levels of inhibition at higher concentrations of MMPIP.

cAMP Inhibition Studies. Cells were plated in a poly(D-lysine)-coated 96-well plate 1 day before assay. After serum-starving for 2 h, cells were equilibrated using DMEM, 20 mM HEPES, and 0.025% ascorbic acid for 10 min at room temperature. Cells were then incubated with 500 μM 3-isobutyl-1-methylxanthine and antagonist or appropriate vehicle for 30 min at 37°C. Forskolin (15 μM) and/or increasing concentrations of L-AP4 were then added to cells and incubated at 37°C for an additional 20 min. Drug solutions were decanted from cells, and 3% trichloroacetic acid was added for >2 h at 4°C to extract intracellular cAMP. Samples were then incubated with bovine protein kinase A and [^{3}H]cAMP (1 nM) for 2 h on ice. After harvesting samples onto a GF/B filter plate (PerkinElmer Life and Analytical Sciences, Waltham, MA), samples were counted in a Packard TopCount (PerkinElmer Life and Analytical Sciences), and [cAMP] in each sample was determined based on a standard curve of unlabeled cAMP.

Epic Experiments. Rat mGluR7a/HEK cells were plated at a density of 7500 cells/well in a 20-μl volume in a fibronectin-coated Epic plate (Corning Life Sciences, Lowell, NY) in assay medium. The following day, the medium was removed, and cells were incubated in 40 μl of buffer (Hanks' balanced salt solution, 20 mM HEPES, and 0.05–0.5% DMSO depending on the experiment). Plates were incubated for 2 h at 26°C, and a baseline reading was taken every 1.5 min for 4.5 min. Plates were removed, and 10 μl of 5× ligand was then added to all wells of the plate simultaneously using the automated liquid handling pipettor of the Hamamatsu FDSS6000, and the plate was returned to the Epic reader. Readings were taken every 1.5 min for a total read period of 50 min. The magnitude of the wavelength shift recorded by the Epic, measured in picometers, at a particular time point was then extracted from the data trace, and the resulting concentration-response curves were fitted to a four-parameter logistic equation using GraphPad Prism 4.0.

Electrophysiology. Adult male Sprague-Dawley rats (Charles River Laboratories, Inc., Wilmington, MA) were anesthetized with isoflurane, decapitated, and the brains were quickly removed and submerged into ice-cold cutting solution (110 mM sucrose, 60 mM NaCl, 3 mM KCl, 1.25 mM NaH_2PO_4, 28 mM $NaHCO_3$, 5 mM glucose, 0.6 mM (+)-sodium-L-ascorbate, 0.5 mM $CaCl_2$, and 7 mM $MgCl_2$) continuously bubbled with 95% O_2/5% CO_2. The brains were then hemisected, and 400-μm transverse slices were made using a Vibratome (Leica VT100S; Leica Microsystems, Inc., Deerfield, IL). Individual hippocampi were removed from the slice and transferred to a room-temperature mixture containing equal volumes of cutting solution and artificial cerebrospinal fluid (ACSF; 125 mM NaCl, 2.5 mM KCl, 1.25 mM NaH_2PO_4, 25 mM $NaHCO_3$, 25 mM glucose, 2 mM $CaCl_2$, and 1 mM $MgCl_2$), where they were allowed to equilibrate for 30 min. The hippocampi were then placed into a holding chamber containing room-temperature ACSF continuously bubbled with 95% O_2/5% CO_2 and allowed to recover for at least 1 h.

After recovery, slices were moved to a submersion chamber continuously perfused with oxygenated ACSF at a rate of 1.5 ml/min. ASCF temperature was maintained between 24 and 25°C. Drugs were diluted to the appropriate concentrations in either −DMSO (<0.1%) plus ACSF or ACSF equilibrated with 95% O_2/5% CO_2 and applied to the slice through the perfusion medium. Field excitatory postsynaptic potentials (fEPSPs) were evoked at 0.05 Hz by placing a bipolar nickel/chromium-stimulating electrode in the stratum radiatum near the CA3–CA1 border to stimulate the Schaffer collaterals. Baseline intensities that evoked half-maximal fEPSPs were chosen for all experiments. Recording electrodes were pulled on a Flaming/Brown micropipette puller (Sutter Instrument Company, Novato, CA) to a resistance of 4 to 5 MΩ, filled with ACSF, and placed in the stratum radiatum of area CA1. Field potentials were recorded using a Warner Instruments PC-505B amplifier (Warner Instruments, Hamden, CT) and analyzed using Clampex 9.2 (Molecular Devices, Sunnyvale, CA). Sampled data were analyzed off-line using Clampfit 9.2 (Molecular Devices). Three sequential fEPSPs were averaged, and their were slopes calculated. All fEPSP slopes were normalized to the average slope calculated during the predrug period (percentage of predrug).

Synthesis of MMPIP and Analogs. Synthesis of MMPIP and analogs is described in detail in the Supplemental Chemistry Methods material.

Chemicals. L-AP4 was purchased from Ascent Scientific (Princeton, NJ), and LY341495 and glutamate were purchased from Tocris Bioscience (Ellisville, MO).

Results

MMPIP and Its Analogs Antagonize Responses in Rat mGluR7/Gα_{15}-Expressing Cells. We synthesized MMPIP, and approximately 40 structurally related analogs to determine the effects of these compounds on mGluR7. At first, activities of MMPIP-derived compounds were evaluated by determining their effects in BHK cells coexpressing mGluR7a and the promiscuous G protein Gα_{15}. Although mGluR7 is typically believed to couple primarily to $G_{i/o}$ and associated signaling pathways (Saugstad et al., 1994; Wu et al., 1998), this receptor can also couple via Gα_{15} to induce increases in intracellular calcium mobilization (Corti et al., 1998; Suzuki et al., 2007). Consistent with previous results (Suzuki et al., 2007), MMPIP inhibited calcium mobilization responses induced by the orthosteric mGluR7 agonist L-AP4 with an IC_{50} of 70.3 ± 20.4 nM (mean ± S.E.M.; Fig. 1A). In addition, L-AP4 concentration-response curves performed in the presence of increasing concentrations of MMPIP revealed a progressive decrease in the maximal L-AP4 response with little change in L-AP4 potency, consistent with a noncompetitive mechanism of action and similar to the findings of Suzuki et al. (2007) (Fig. 1B).

Synthesis and screening of analogs of MMPIP revealed that several compounds exhibited similar inhibitory effects

on mGluR7-mediated calcium responses (Fig. 2A). It is noteworthy that concentration-response analyses revealed that two analogs of MMPIP examined in more detail, VUSC001 and VUSC027, exhibited similar potencies to that of MMPIP itself (79.5 ± 11.8 and 49.2 ± 21 nM, respectively, mean ± S.E.M.) but exhibited saturable, yet incomplete, levels of antagonism of mGluR7-mediated responses induced by a concentration of agonist eliciting an 80% maximal response (maximal percentage blockade: MMPIP, 100.7 ± 1.1%; VUSC001, 83.2 ± 4.1%; VUSC027, 62.3 ± 7.0%; Fig. 2B). These results are similar to studies reported previously with mGluR5 NAMs based on the MPEP scaffold (Rodriguez et al., 2005). This suggests that NAMs in the MMPIP series exhibit a range of abilities to affect agonist-mediated calcium responses induced by L-AP4.

MMPIP and Its Analogs Are Less Active in Inhibiting mGluR7 Regulation of GIRK Channels Compared with mGluR7-Induced Calcium Mobilization. Chimeric and promiscuous G proteins are often used as surrogate strategies to more easily assess the activity of GPCRs that might be difficult to measure using other techniques or in high-throughput format. mGluR7 is not believed to couple to $G\alpha_{15}$ in native systems but has been shown to couple to endogenous $G_{i/o}$ G proteins within different cellular backgrounds, including neurons, to induce downstream responses (Saugstad et al., 1994, 1996; Wu et al., 1998; Lafon-Cazal et al., 1999). We recently developed a multiwell plate assay to assess mGluR7-mediated $G_{i/o}$-dependent responses (Niswender et al., 2008). This assay is based on the ability of $G_{i/o}$ G proteins to interact with ion channels via $G\beta\gamma$ subunits and measures the flux of the ion thallium through GIRK channels. When analogs of MMPIP were screened using this assay, it was observed that all MMPIP analogs showed weaker activity in inhibiting GIRK responses compared with their activities in the calcium mobilization assay (Fig. 3A versus 2A).

The finding that a single concentration of MMPIP does not completely antagonize the GIRK response at a concentration that completely blocks the calcium mobilization response to mGluR7 activation could be due to a number of factors, including differential potencies at inhibiting the two responses, different levels of negative cooperativity, distinct cell backgrounds, or a combination of these. We next performed full concentration-response analyses of MMPIP using mGluR4, mGluR7, mGluR8, and M4 muscarinic receptor-expressing cell lines. High concentrations of MMPIP inhibited thallium flux in multiple cell lines, including the unre-

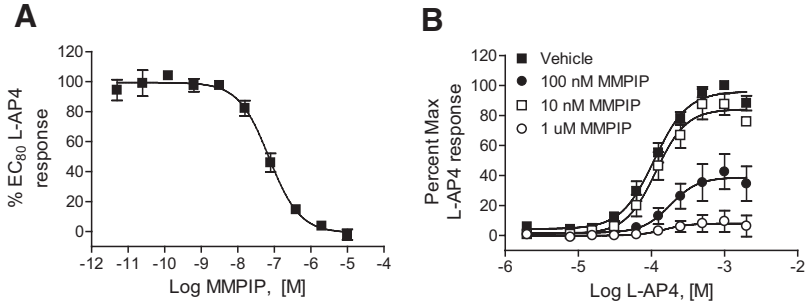

Fig. 1. MMPIP antagonizes responses in mGluR7/BHK/$G\alpha_{15}$ cells in a noncompetitive fashion. A, cells coexpressing rat mGluR7a and the promiscuous G protein $G\alpha_{15}$ were incubated with increasing concentrations of MMPIP before the addition of an EC_{80} concentration of the group III mGluR agonist L-AP4, and calcium mobilization was measured. EC_{50} = 70.3 ± 20.4 nM. B, L-AP4 concentration-response curves were performed in the presence of increasing concentrations of MMPIP. Values represent mean ± S.E.M. of three independent experiments performed in quadruplicate.

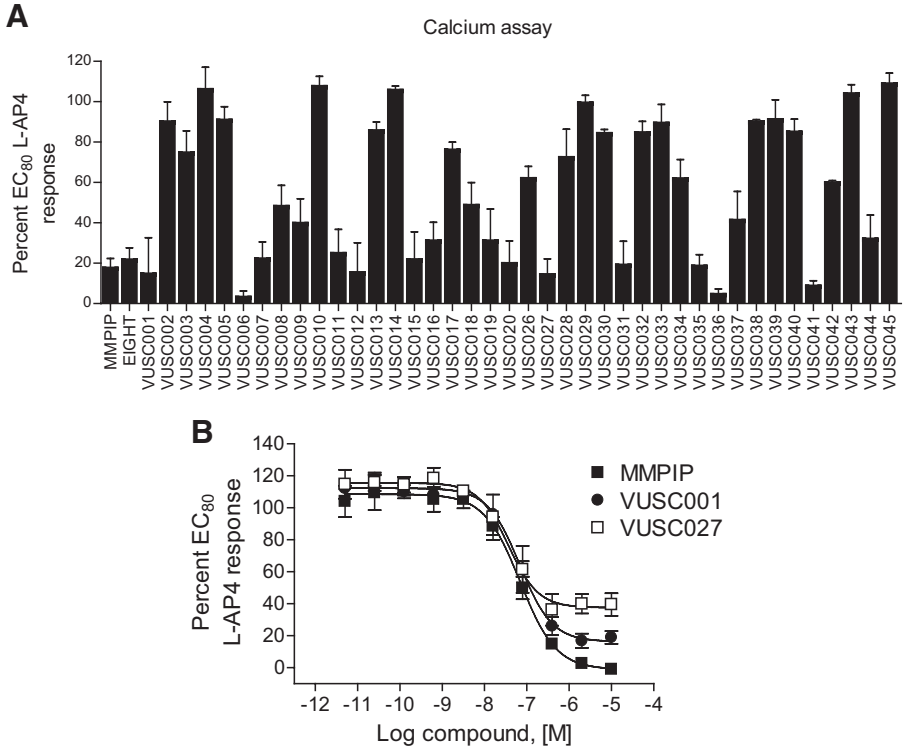

Fig. 2. MMPIP analogs exhibit a range of efficacies for inhibition of mGluR7-mediated calcium mobilization. A, compounds were preapplied to mGluR7a/BHK/$G\alpha_{15}$ cells before the addition of an EC_{80} concentration of L-AP4, and calcium mobilization was measured. B, selected compounds were assessed in full concentration-response format for the inhibition of mGluR7-mediate calcium mobilization. MMPIP data are replotted from Fig. 1B for comparison. Potencies were as follows: VUSC001, 79.5 ± 11.8 nM; VUSC027, 49.2 ± 21.0 nM. Maximal inhibition values for each compound (calculated the lowest point of the curve fit as determined using a four site logistical equation in GraphPad Prism) were as follows: MMPIP, 100.7 ± 1.1%, VUSC001, 83.1 ± 4.1%; and VUSC027, 62.3 ± 7.0%. Values represent the mean ± S.E.M. of at least three experiments performed in quadruplicate.

lated M4 muscarinic receptor (Fig. 3B), suggesting that high concentrations most likely inhibit GIRK potassium channel activity directly or inhibit other cellular components that contribute to overall thallium flux. After correction for potential nonspecific effects of high MMPIP concentrations as outlined under *Materials and Methods*, concentration-response curve analyses of corrected thallium flux traces revealed that MMPIP was ~10-fold less potent in inhibiting mGluR7-induced GIRK activation compared with inhibition of agonist-mediated calcium mobilization (718 ± 90 versus 70.3 ± 20.4 nM, mean ± S.E.M.; Figs. 3C versus 1A). At maximally effective concentrations, MMPIP induced only a 44.5 ± 4% inhibition of the EC_{80} L-AP4 response. In contrast, previous studies from our laboratory have shown that the orthosteric antagonist LY341495 completely blocks L-AP4-induced responses in the mGluR7 thallium flux assay (Niswender et al., 2008).

Because of the low affinity and efficacy of glutamate at mGluR7, L-AP4 is often used as a surrogate agonist. In addition, in electrophysiology studies, L-AP4 is commonly used as a selective group III mGluR agonist rather than glutamate because glutamate activates all mGluRs as well as ionotropic receptors and glutamate transporters. Because it is well known that the effects of allosteric ligands are highly dependent on the agonist, or "probe" used for receptor activation (Leach et al., 2007), we next determined whether the low activity of MMPIP in the thallium flux assay would extend to studies in which glutamate was used as the agonist. In these experiments, glutamate induced approximately 20% of the maximal response induced by L-AP4 (data not shown). When agonist responses in the presence and absence of 1 μM MMPIP were normalized for each relative agonist response, the maximal blockade induced by MMPIP was not significantly different for the two agonists (Fig. 4A, 71 ± 3.8% inhibition, L-AP4; 4B, 67.7 ± 6.8% inhibition, glutamate, mean ± S.E.M.). These results suggest that the reduced effect of MMPIP in inhibiting GIRK activity is independent of the use of L-AP4 or glutamate.

MMPIP Does Not Block L-AP4-Induced Inhibition of cAMP Accumulation in mGluR7/HEK Cells. Differential effects of MMPIP on mGluR7-mediated calcium mobilization versus modulation of GIRK suggest that MMPIP and related

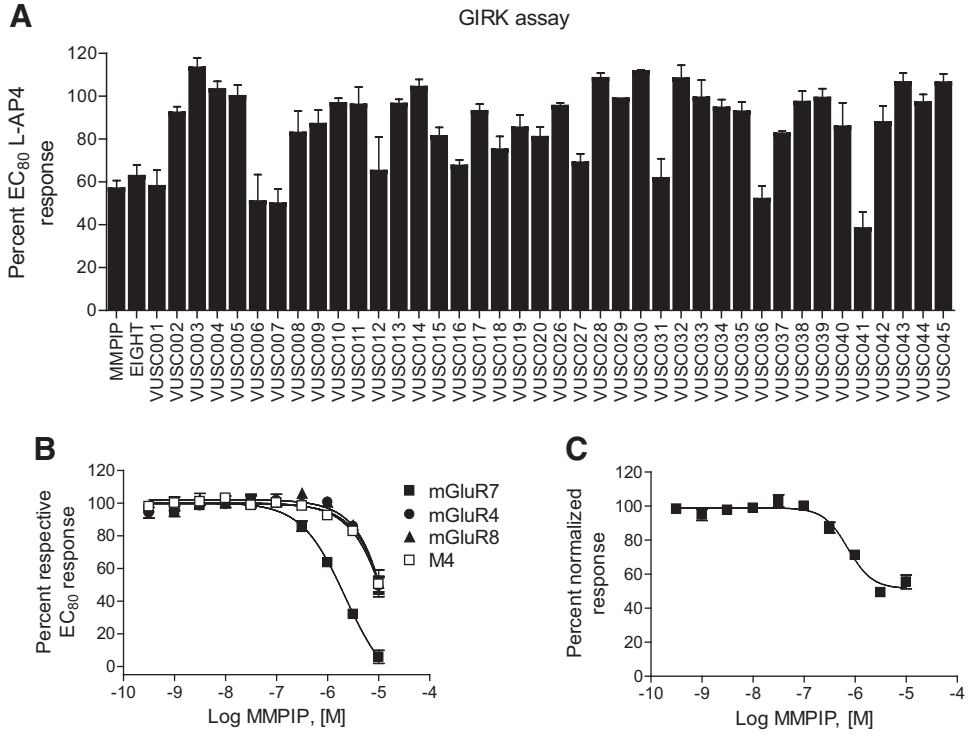

Fig. 3. MMPIP analogs exhibit lower efficacies in thallium flux assays, and the potency of MMPIP is lower than in calcium mobilization studies. A, compounds were preapplied to mGluR7a/HEK/GIRK cells before the addition of an EC_{80} concentration of L-AP4, and thallium flux through the GIRK channel was measured. B, MMPIP concentration-response in thallium flux assays using cells expressing mGluR4, mGluR7, mGluR8, and M4 muscarinic receptor. In each case, concentration-response curves were applied to cells before an appropriate EC_{80} concentration of either L-AP4 (mGluR4, 7, and 8) or acetylcholine (M4). The potency of MMPIP in these experiments was 2.0 ± 0.2 μM. C, corrected concentration-response curve for MMPIP after normalizing for nonspecific effects of the compound on M4/GIRK cells. Methods for this correction are described under *Materials and Methods*. Revised potency of MMPIP, 717 ± 89 nM. Values represent mean ± S.E.M. and are an *n* of three experiments performed in quadruplicate.

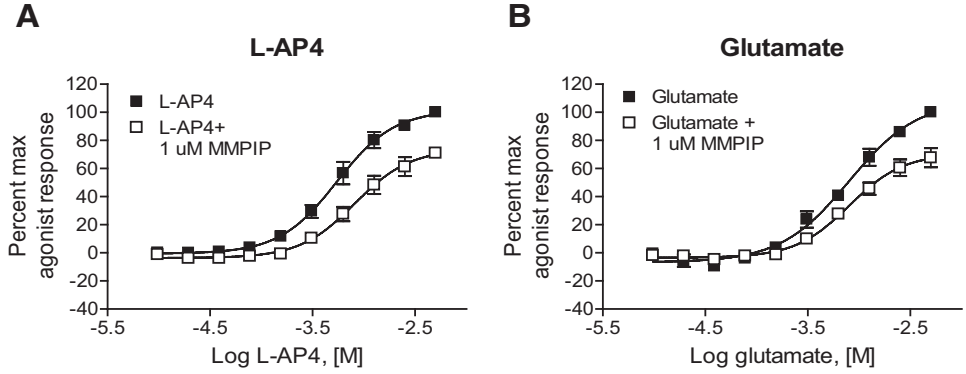

Fig. 4. The level of MMPIP blockade is not probe-dependent in the GIRK/thallium flux assay. A 1 μM final concentration of MMPIP was preapplied before the addition of increasing concentrations of L-AP4 (A) or glutamate (B), and thallium flux was measured. The response remaining was 71 ±3.8% for L-AP4 (A) and 67.7 ± 6.8%, glutamate. Data represent the mean ± S.E.M. of three independent experiments performed in quadruplicate.

compounds differentially modulate mGluR7 depending on the signaling pathway or cellular context in which responses are measured. We next decided to focus on the study of the mGluR7/HEK cell line used for the thallium flux experiments. If MMPIP was selective in its ability to block specific signaling pathways, assessing different signaling events in the same cell background was critical to define this as the mechanism. If the blockade induced by MMPIP was context-dependent, in contrast, we would predict that MMPIP would exhibit similar pharmacology in blocking various mGluR7/HEK cell responses, which might differ globally from responses seen in cell background, such as BHK cells.

The GIRK assay measures the readout downstream of the G$\beta\gamma$ subunits of the G protein, suggesting that it was formally possible that MMPIP exhibited differential ability to block these responses versus those modulated by the Gα subunits of the heterotrimeric G protein. To further evaluate the effects of MMPIP on another response that is mediated by endogenous $G_{i/o}$ and to assess the ability of the compound to block a Gα-mediated response, we performed studies of effects of MMPIP on mGluR7-mediated inhibition of cAMP accumulation in mGluR7/HEK cells. As reported previously (Suzuki et al., 2007), MMPIP increased cAMP accumulation when added in the absence of L-AP4 (Fig. 5A; EC_{50}, 690 ± 130 nM). This effect of MMPIP on basal cAMP accumulation made it difficult to interpret the level of blockade induced by a single concentration of L-AP4 (data not shown). For this reason, we performed full concentration-response analyses of L-AP4 in the presence and absence of 1 μM MMPIP, a concentration that was maximally effective in calcium mobilization assays. MMPIP induced a large increase in cAMP levels alone but did not significantly block L-AP4-induced inhibition of cAMP accumulation (Fig. 5B). In contrast, the orthosteric antagonist LY341495 completely blocked L-AP4-induced inhibition of cAMP accumulation with no change in forskolin-stimulated cAMP levels alone (Fig. 5B). These data suggested that, compared with responses in BHK cells, MMPIP demonstrated reduced negative cooperativity in blocking two pathways when mGluR7 was expressed in HEK cells, one downstream of G$\beta\gamma$ subunits and one downstream of Gα subunits. These data provided further evidence for context-dependence of MMPIP action on mGluR7.

MMPIP Exhibits Context-Dependent, Saturable Effects on mGluR7 Activity Using an Additional Phenotypic Assay of mGluR7 Function. One difference between the effects measured between BHK cells and HEK cells is the nature of the G protein used for signal transduction. For example, it is possible that MMPIP may be more effective at inhibiting responses that are mediated by the coupling of mGluR7 to a promiscuous G protein than to endogenous $G_{i/o}$. In contrast, MMPIP effects may be dependent on the cell background in which the receptor is expressed. To more directly compare the effects of MMPIP on responses to mGluR7 activation between cellular backgrounds, we measured mGluR7 activity using a novel phenotypic assay of GPCR function (Epic; Corning). This technique relies on plating cells expressing the receptor of interest onto a plate in which individual wells contain a resonance waveguide grating. Initial baseline readings are taken by illuminating the plate with a broadband light source and measuring the wavelength of the refracted light. After cell stimulation, mass redistribution of intracellular components occurs, resulting in a shift in the refracted wavelength. Responses are measured as a picometer wavelength shift from the initial recorded wavelength and can occur in either a positive or negative direction. Rather than reflecting the effects of receptor activation on a single signaling pathway, this assay is believed to provide a measure of effects on a composite of different signaling responses to a GPCR ligand, although certain pathways presumably dominate the measured kinetic trace. L-AP4 induced concentration-dependent wavelength shifts in both mGluR7/BHK/Gα_{15} and mGluR7/HEK cells using the Epic system (Fig. 6A, effects of L-AP4 alone in mGluR7/HEK cells are shown). L-AP4 was equipotent in inducing Epic responses in mGluR7 BHK and mGluR7/HEK cells (Fig. 7, A: mGluR7/BHK, L-AP4 EC_{50}, 177 ± 51 μM; B: mGluR7/HEK, L-AP4 EC_{50}, 195 ± 60 μM, mean ± S.E.M.). These L-AP4 responses were blocked in both cell lines by pertussis toxin (data not shown), a compound that prevents signaling through $G_{i/o}$ proteins. This suggests that the L-AP4 responses in both cell lines using the Epic readout are mediated by $G_{i/o}$ proteins rather than, for the BHK cell line, Gα_{15}; this might be expected because Gα_{15} couples weakly to mGluR7 (Corti et al., 1998) and our calcium responses in this cell line are detectable but extremely small compared with native or overexpressed G_q-coupled receptors (data not shown). As with the cAMP measurements, MMPIP clearly induced responses alone; these responses were concentration-dependent, seemed to be specific to mGluR7 because there was no corresponding response in mGluR4-expressing

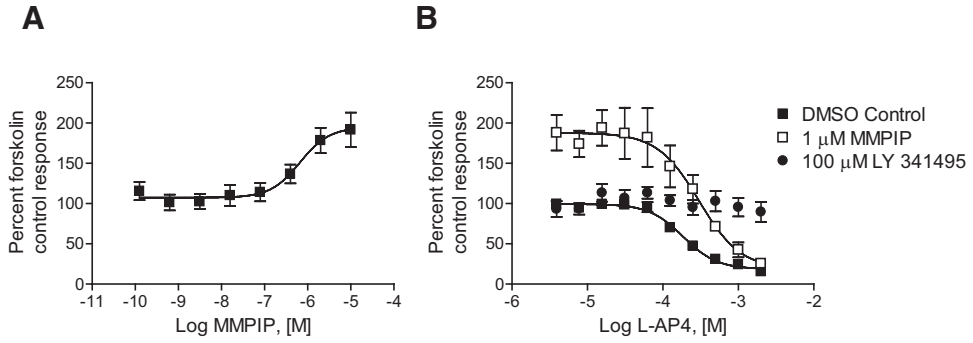

Fig. 5. MMPIP raises basal cAMP levels and fails to effectively block L-AP4-mediated inhibition of cAMP accumulation. A, MMPIP induced a concentration-dependent increase in cAMP accumulation in mGluR7/HEK cells (EC_{50} = 690 ± 130 nM). B, in contrast to blockade obtained in the presence of 100 μM concentration of the orthosteric antagonist LY341495 (●), a 1 μM concentration of MMPIP (□) increased basal cAMP levels but did not effectively block L-AP4-mediated inhibition of cAMP accumulation (compared maximal blockade to curve of L-AP4 alone, ■). Data represent the mean ± S.E.M. of three independent experiments performed in triplicate.

cells (Fig. 7C), and the wavelength shifts were in the opposite direction of those induced by L-AP4 (representative example of traces shown in Fig. 6B; resulting concentration-response curve for mGluR7/HEK cells are shown as ■ in Fig. 7C). Concentration-response curves of L-AP4 in the presence of 1 μM MMPIP were, again, very different between the two cell lines, with much more robust inhibition being observed in mGluR7/BHK cells compared with mGluR7/HEK cells (Fig. 7, A versus B). Concentration-response curves of MMPIP in the presence of an EC_{80} concentration of L-AP4, when corrected for responses obtained in the presence of the compound alone, again revealed distinct levels of inhibition between the two cell lines (Fig. 7D). It is significant that these concentration-response curves were saturable, suggesting that these effects are not due to differences in receptor expression between the two cell lines. A fit of the normalized data revealed that MMPIP blocked responses in mGluR7/HEK cells by 46.0 ± 1.8% with a potency of 156 ± 28 nM (Fig. 7D; mean ± S.E.M., n = 3). This level of inhibition was remarkably similar to the effect observed in the thallium flux assay when the data were corrected for nonspecific effects (44.5 ± 4%). In contrast, in mGluR7/BHK cells, MMPIP was exhibited a potency similar to that observed in the calcium assay and increased maximal blockade compared with mGluR7/HEK cells (75.2 ± 3.3% blockade, 50 ± 15 nM; mean ± S.E.M., n = 3).

MMPIP Is Ineffective at Blocking L-AP4-Mediated Reductions of Synaptic Transmission at the Schaffer Collateral-CA1 Synapse. In its native environment, mGluR7 is predominantly expressed in presynaptic terminals of excitatory glutamatergic synapses (Shigemoto et al., 1997) where it is believed to serve as an autoreceptor to inhibit glutamate release. The actions of group III mGluR activation have been most rigorously evaluated at a glutamatergic synapse in the hippocampal formation termed the Schaffer collateral-CA1 (SC-CA1) synapse (Baskys and Malenka, 1991; Gereau and Conn, 1995; Ayala et al., 2008). Activation of mGluR7 with L-AP4 reduces evoked excitatory postsynaptic potentials (EPSPs) at this synapse, and evidence suggests that there is no contribution of mGluR4 or mGluR8 to the response to L-AP4 at the SC-CA1 synapse in adult animals (Ayala et al., 2008). To assess the effect of MMPIP on mGluR7 activity in a native system, we determined the effects of this compound on L-AP4-induced modulation of transmission at the SC-CA1 synapse. Consistent with previous reports, L-AP4 (400 μM) reduced the initial slope of fEPSPs recorded at the SC-CA1 synapse. The concentration of L-AP4 used was chosen based on L-AP4 concentration-response curves, showing that this concentration elicits a robust but submaximal response. Consistent with our previous reports (Ayala et al., 2008), the orthosteric antagonist LY341495 significantly blocked L-AP4-mediated reduc-

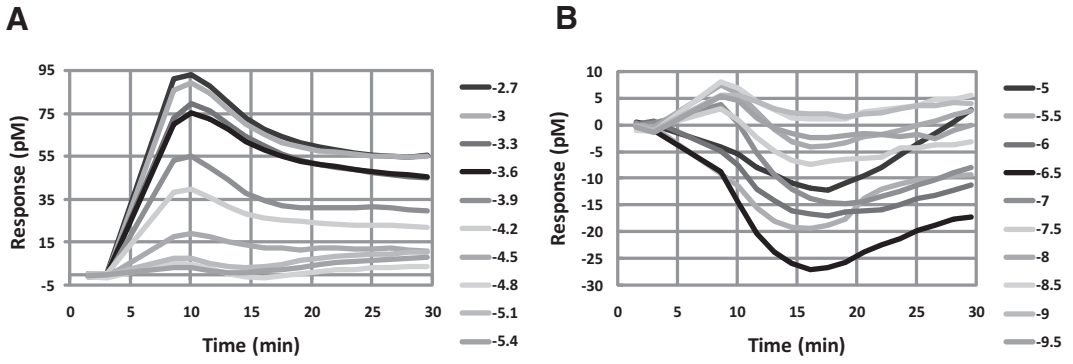

Fig. 6. L-AP4 and MMPIP induce opposing responses in mGluR7/HEK cells using Epic technology. mGluR7/HEK cells were plated into 384-well Epic plates as described under *Materials and Methods*. Increasing concentrations of L-AP4 (A) or MMPIP (B) were applied to cells, and Epic responses were measured.

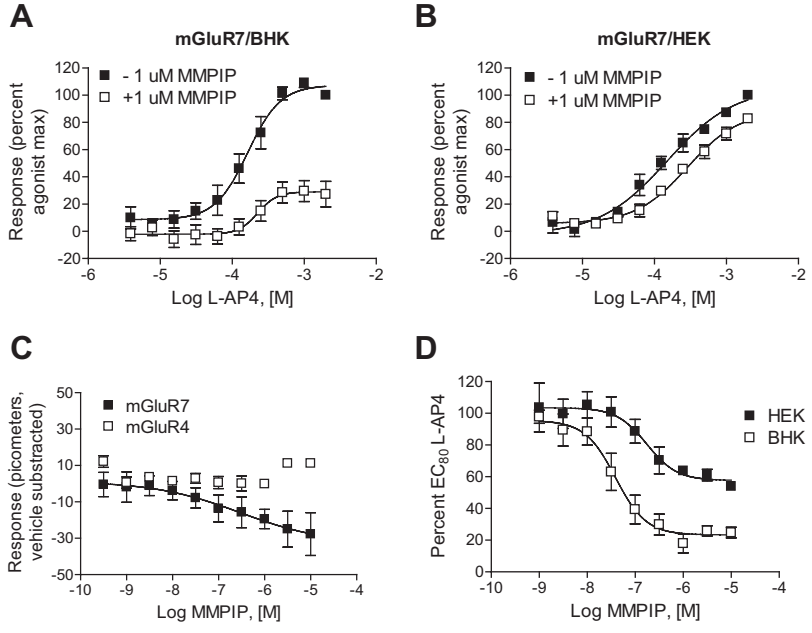

Fig. 7. MMPIP antagonizes L-AP4 responses at mGluR7 with distinct and saturable efficacies in mGluR7/HEK and mGluR7/BHK cells as assessed using Epic technology. Increasing concentrations of L-AP4 were added to mGluR7/BHK (A) or mGluR7/HEK (B) cells in the presence (□) and absence (■) of 1 μM MMPIP and the responses, measured as a change in refractive index indicative of cellular mass distribution, were determined. C. increasing concentrations of MMPIP were incubated with mGluR7/HEK (■) or mGluR4/HEK (□) cells in the absence of agonist. MMPIP induced decreases in refractive index in cells expressing mGluR7 but not cells expressing mGluR4. D, increasing concentrations of MMPIP were incubated with mGluR7/BHK (●) mGluR7/HEK (○) cells in the absence or presence of an EC_{80} concentration of L-AP4. Individual responses in the presence of L-AP4 were subtracted by the response induced by MMPIP in the absence of L-AP4. The potency of MMPIP in mGluR7/BHK cells was 50 ± 15 nM and in mGluR7/HEK cells was 156 ± 28 nM. The percentage of maximal blockade was 75.2 ± 3.3% in mGluR7/BHK cells and 46.0 ± 1.8% in mGluR7/HEK cells Data for each panel represent mean ± S.E.M. of three independent experiments performed in quadruplicate.

tions in neurotransmission (Fig. 8, A and C). In contrast, MMPIP, at a 10 μM concentration (approximately 100 times higher than the IC_{50} in in vitro calcium assay experiments), was not effective in blocking the effects of L-AP4 on transmission at this synapse (Fig. 8, B and D). Overall, the combination of in vitro pharmacology and electrophysiology results suggest that MMPIP exhibits differential degrees of negative cooperativity in different cellular contexts and is ineffective at antagonizing mGluR7 activity at a central glutamatergic synapse that is believed to reflect one of the major physiological roles of this GPCR in the CNS.

Discussion

Until recently, the focus of most GPCR ligand discovery programs has been on the development of orthosteric ligands. Allosteric compounds have begun to emerge as a potentially useful strategy by which to modulate receptor function, and these ligands possess several advantages (Conn et al., 2009). For example, many orthosteric ligands are based on chemical scaffolds that are difficult to optimize as drug candidates with ideal pharmacokinetic properties; in contrast, allosteric ligands are often amenable to chemical optimization. Furthermore, allosteric ligands often exhibit a high degree of selectivity for a particular receptor over closely related subtypes. In addition, PAMs, which often have no effect on their own but instead act by potentiating the effects of the orthosteric ligand, have the ability to maintain the temporal and spatial activity of the endogenous agonist. Although potential advantages of maintaining activity-dependence are largely theoretical, examples are beginning to emerge in which PAMs provide more physiologically appropriate increases in receptor function than is seen with traditional agonists (Ayala et al., 2008).

As the development of allosteric ligands has grown, so has the appreciation of their underlying pharmacology. Because these compounds bind to alternate sites on a GPCR compared with the endogenous ligand, it might be expected that they could place the receptor in a unique structural conformation that might not be achieved, or at least favored, in their absence. This could result in preferential regulation of certain pathways in the presence of an allosteric ligand. For example, the allosteric modulator *N*-{4-chloro-2-[(1,3-dioxo-1,3-dihydro-2H-isoindol-2-yl)methyl]phenyl}-2-hydroxybenzamide exhibits differential effects on calcium mobilization and extracellular signal-regulated kinases 1/2 phosphorylation downstream of mGluR5 activation in cultured cortical astrocytes (Zhang et al., 2005). As an example of complex pharmacology induced by NAMs, 1-(4-ethoxyphenyl)-5-methoxy-2-methylindole-3-carboxylic acid is an allosteric modulator of the chemoattractant-receptor-homologous molecule, CRTH2, on T-helper 2 cells. This compound has been shown to be inactive against prostaglandin D2-induced G protein-linked pathways but acts as a potent antagonist of G protein-independent, β-arrestin coupling to the same receptor (Mathiesen et al., 2005).

The compound presented here, MMPIP, may best be referred to as exhibiting "context- dependent" pharmacology. MMPIP was discovered using a CHO cell line in which the promiscuous G protein $G\alpha_{15}$ was coexpressed to induce calcium mobilization (Suzuki et al., 2007). We generated a similar cell line by using Ga15 and replicated the findings of Suzuki et al., including the observation that MMPIP seemed to act via a noncompetitive mechanism of action, suggesting that MMPIP behaves similarly when mGluR7 is expressed in either CHO or BHK backgrounds. However, further analysis of the effects of MMPIP and analogs revealed activities consistent with a range of negative cooperativities induced by members of this structural class in the calcium mobilization assay. Movement to a different cell background revealed that MMPIP showed weaker potency and efficacy in inhibiting mGluR7 modulation of GIRK potassium channels and was essentially devoid of antagonist activity in blocking mGluR7-mediated inhibition of cAMP accumulation in contrast to its apparent inverse agonist effects. These experiments were designed to assess either $G\beta\gamma$ or $G\alpha$-mediated signaling arms of $G_{i/o}$ proteins and are consistent with MMPIP showing reduced negative cooperativity in the HEK cell, compared with the BHK cell, background. Finally, MMPIP exhibited

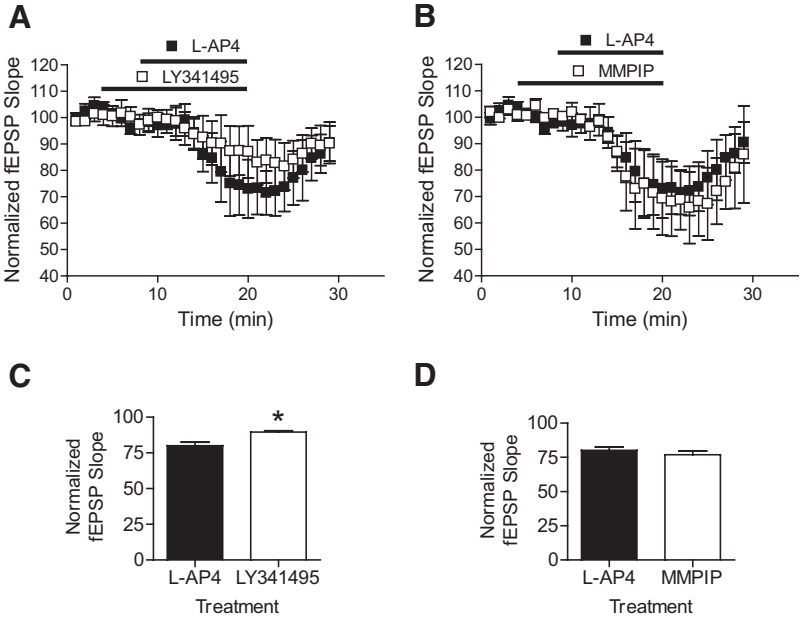

Fig. 8. MMPIP does not block L-AP4-mediated depression of synaptic transmission at the Schaffer collateral-CA1 synapse. fEPSPs were measured at the SC-CA1 synapse in adult rat hippocampus. A, the effect of a submaximal concentration of L-AP4 on fEPSP slope (400 μM) over time is shown (dark symbols). This response was significantly blocked by a 5-min preincubation with 100 μM LY341495 (open symbols). After normalizing for responses across slices, the maximal effect of LY341495 over a 5-min period was quantified as shown in Fig. 8C (*, $p = 0.0065$). B, a 5-min preincubation with 10 μM MMPIP before L-AP4 addition had no significant effect on fEPSP slope (quantified in D). Data are from four to five slices derived from two to three animals.

differential but saturable abilities to block L-AP4-induced signals in different cell lines assessed using Epic technology, an assay that can be used to compare integrated receptor signaling events in different cellular backgrounds. Preliminary results suggest that the differential effects observed were not due to the presence of $G\alpha_{15}$ in the BHK cell line as the response was blocked by the $G_{i/o}$ inactivator pertussis toxin (data not shown). We note, however, that the blockade in the BHK cell line does saturate at approximately 75% blockade versus the 100% blockade seen in calcium responses. Therefore, there may still be distinctions in signaling that depend on the G protein mediating the response with potential distinctions in signaling between $G\alpha_{15}$ (for calcium mobilization) and $G_{i/o}$ (for Epic). In addition, the $G_{i/o}$ complement between HEK and BHK cells may differ, which could also contribute to the differences seen between the two cell lines.

In contrast to LY341495, MMPIP did not block mGluR7-mediated depression of transmission at the SC-CA1 synapse. Although this does not necessarily imply that MMPIP will be ineffective at blocking all mGluR7 responses in native systems, previous studies suggest that the predominant role of mGluR7 in the CNS is to act as an autoreceptor involved in reducing transmission at glutamatergic synapses via $G_{i/o}$-mediated signaling. Thus, it is possible that MMPIP will have relatively little effect on this important response to mGluR7 at other central synapses. MMPIP exhibited similar effects on L-AP4 versus glutamate-mediated thallium flux, suggesting that MMPIP will also exhibit low levels of negative cooperativity in blocking certain glutamate-mediated effects in vivo. In future studies, it will be important to further evaluate the effects of MMPIP at other synapses and on other responses in CNS preparations. It is interesting that we and others have observed similar context-dependent effects with the allosteric mGluR7 agonist AMN082. AMN082 seems to be capable of activating mGluR7 when measured in some pathways and cell backgrounds but not others (Suzuki et al., 2007; Ayala et al., 2008; C. M. Niswender, unpublished observations). It is noteworthy that AMN082 is similar to MMPIP in that this compound is without effect at the SC-CA1 synapse (Ayala et al., 2008), further suggesting complexity in mGluR7 ligand pharmacology in terms of both NAMs and allosteric activators.

The finding that the context of expression of mGluR7 plays a critical role in its function and pharmacology is, perhaps, not unexpected based on studies exploring the regulation of mGluR7 by intracellular interacting proteins. The mGluR7 C-terminal tail binds to a variety of interacting proteins such as the clustering protein PICK1 (protein interacting with C kinase 1) (Dev et al., 2001; El Far and Betz, 2002). PICK1 also binds protein kinase Cα, and the three proteins form a complex at the active zones of presynaptic terminals (El Far and Betz, 2002). In addition, mGluR7a interacts with Ca^{2+}/calmodulin, G protein $\beta\gamma$ subunits, and the protein macrophage myristoylated alanine-rich *C* kinase *s*ubstrate via the C-terminal tail region (Bertaso et al., 2006). It has been hypothesized that this complex signaling system, coupled with the low affinity of mGluR7 for glutamate, may provide a way to ensure that mGluR7 is only activated during periods of intense synaptic activity and allow the receptor to serve as an integrator of multiple presynaptic signaling events, including increases in intracellular calcium.

Bertaso et al. (2008) recently described an elegant set of studies in which the mGluR7a-PICK1 interaction was disrupted by using a viral vector in which the last nine amino acids of the C terminus of mGluR7 were used as "bait" to compete with full-length receptor-PICK1 binding. Infection of neurons with this construct in vivo inhibited mGluR7-PICK1 interactions and led to absence seizures and electroencephalogram wave form changes specifically within thalamocortical brain regions. It is interesting that mGluR7 modulation effects induced by viral infection seemed to be specific to thalamocortical circuits, and mGluR7 activity in the hippocampus, as assessed by c-fos immunostaining or electroencephalogram recordings, was not affected. These findings suggest that it is possible that protein-protein interactions or the cellular context in which those protein interactions occur may affect mGluR7 activity in vivo and raise the intriguing possibility that the pharmacology of ligands interacting with this receptor may be intimately regulated by protein-protein interactions. It will be of interest to further explore these interactions and determine their implications for mGluR7-based drug design and development because this receptor is a key target for numerous CNS disorders such as epilepsy and anxiety (Niswender et al., 2005).

Acknowledgments

We thank Dr. Karen Gregory for comments on the manuscript.

References

Ayala JE, Niswender CM, Luo Q, Banko JL, and Conn PJ (2008) Group III mGluR regulation of synaptic transmission at the SC-CA1 synapse is developmentally regulated. *Neuropharmacology* **54:**804–814.

Baskys A and Malenka RC (1991) Agonists at metabotropic glutamate receptors presynaptically inhibit EPSCs in neonatal rat hippocampus. *J Physiol* **444:**687–701.

Bertaso F, Lill Y, Airas JM, Espeut J, Blahos J, Bockaert J, Fagni L, Betz H, and El-Far O (2006) MacMARCKS interacts with the metabotropic glutamate receptor type 7 and modulates G protein-mediated constitutive inhibition of calcium channels. *J Neurochem* **99:**288–298.

Bertaso F, Zhang C, Scheschonka A, de Bock F, Fontanaud P, Marin P, Huganir RL, Betz H, Bockaert J, Fagni L, et al. (2008) PICK1 uncoupling from mGluR7a causes absence-like seizures. *Nat Neurosci* **11:**940–948.

Conklin BR, Farfel Z, Lustig KD, Julius D, and Bourne HR (1993) Substitution of three amino acids switches receptor specificity of Gq alpha to that of Gi alpha. *Nature* **363:**274–276.

Conn PJ, Christopoulos A, and Lindsley CW (2009) Allosteric modulators of GPCRs: a novel approach for the treatment of CNS disorders. *Nat Rev Drug Discov* **8:**41–54.

Corti C, Restituito S, Rimland JM, Brabet I, Corsi M, Pin JP, and Ferraguti F (1998) Cloning and characterization of alternative mRNA forms for the rat metabotropic glutamate receptors mGluR7 and mGluR8. *Eur J Neurosci* **10:**3629–3641.

de Rover M, Meye FJ, and Ramakers GM (2008) Presynaptic metabotropic glutamate receptors regulate glutamatergic input to dopamine neurons in the ventral tegmental area. *Neuroscience* **154:**1318–1323.

Dev KK, Nakanishi S, and Henley JM (2001) Regulation of mglu(7) receptors by proteins that interact with the intracellular C-terminus. *Trends Pharmacol Sci* **22:**355–361.

El Far O and Betz H (2002) G-protein-coupled receptors for neurotransmitter amino acids: C-terminal tails, crowded signalosomes. *Biochem J* **365:**329–336.

George SR, O'Dowd BF, and Lee SP (2002) G-protein-coupled receptor oligomerization and its potential for drug discovery. *Nat Rev Drug Discov* **1:**808–820.

Gereau RW 4th and Conn PJ (1995) Multiple presynaptic metabotropic glutamate receptors modulate excitatory and inhibitory synaptic transmission in hippocampal area CA1. *J Neurosci* **15:**6879–6889.

Gilchrist A and Blackmer T (2007) G-protein-coupled receptor pharmacology: examining the edges between theory and proof. *Curr Opin Drug Discov Devel* **10:**446–451.

Groebe DR (2009) In search of negative allosteric modulators of biological targets. *Drug Discov Today* **14:**41–49.

Howard AD, McAllister G, Feighner SD, Liu Q, Nargund RP, Van der Ploeg LH, and Patchett AA (2001) Orphan G-protein-coupled receptors and natural ligand discovery. *Trends Pharmacol Sci* **22:**132–140.

Kenakin T (2005) New concepts in drug discovery: collateral efficacy and permissive antagonism. *Nat Rev Drug Discov* **4:**919–927.

Kenakin T (2008) Functional selectivity in GPCR modulator screening. *Comb Chem High Throughput Screen* **11:**337–343.

Lafon-Cazal M, Fagni L, Guiraud MJ, Mary S, Lerner-Natoli M, Pin JP, Shigemoto R, and Bockaert J (1999) mGluR7-like metabotropic glutamate receptors inhibit

NMDA-mediated excitotoxicity in cultured mouse cerebellar granule neurons. *Eur J Neurosci* **11:**663–672.

Leach K, Sexton PM, and Christopoulos A (2007) Allosteric GPCR modulators: taking advantage of permissive receptor pharmacology. *Trends Pharmacol Sci* **28:**382–389.

Mathiesen JM, Ulven T, Martini L, Gerlach LO, Heinemann A, and Kostenis E (2005) Identification of indole derivatives exclusively interfering with a G protein-independent signaling pathway of the prostaglandin D2 receptor CRTH2. *Mol Pharmacol* **68:**393–402.

Nakamura M, Kurihara H, Suzuki G, Mitsuya M, Ohkubo M, and Ohta H (2010) Isoxozolopyridone derivatives as allosteric metabotropic glutamate receptor 7 antagonists. *Bioorg Med Chem Lett* doi: 10.1016/j.bmcl.2009.11.070.

Niswender CM, Johnson KA, Luo Q, Ayala JE, Kim C, Conn PJ, and Weaver CD (2008) A novel assay of Gi/o-linked G protein-coupled receptor coupling to potassium channels provides new insights into the pharmacology of the group III metabotropic glutamate receptors. *Mol Pharmacol* **73:**1213–1224.

Niswender CM, Jones CK, and Conn PJ (2005) New therapeutic frontiers for metabotropic glutamate receptors. *Curr Top Med Chem* **5:**847–857.

Pelkey KA, Lavezzari G, Racca C, Roche KW, and McBain CJ (2005) mGluR7 is a metaplastic switch controlling bidirectional plasticity of feedforward inhibition. *Neuron* **46:**89–102.

Rodriguez AL, Nong Y, Sekaran NK, Alagille D, Tamagnan GD, and Conn PJ (2005) A close structural analog of 2-methyl-6-(phenylethynyl)-pyridine acts as a neutral allosteric site ligand on metabotropic glutamate receptor subtype 5 and blocks the effects of multiple allosteric modulators. *Mol Pharmacol* **68:**1793–1802.

Saugstad JA, Kinzie JM, Mulvihill ER, Segerson TP, and Westbrook GL (1994) Cloning and expression of a new member of the L-2-amino-4-phosphonobutyric acid-sensitive class of metabotropic glutamate receptors. *Mol Pharmacol* **45:**367–372.

Saugstad JA, Segerson TP, and Westbrook GL (1996) Metabotropic glutamate receptors activate G-protein-coupled inwardly rectifying potassium channels in *Xenopus* oocytes. *J Neurosci* **16:**5979–5985.

Shigemoto R, Kinoshita A, Wada E, Nomura S, Ohishi H, Takada M, Flor PJ, Neki A, Abe T, Nakanishi S, et al. (1997) Differential presynaptic localization of metabotropic glutamate receptor subtypes in the rat hippocampus. *J Neurosci* **17:**7503–7522.

Suzuki G, Tsukamoto N, Fushiki H, Kawagishi A, Nakamura M, Kurihara H, Mitsuya M, Ohkubo M, and Ohta H (2007) In vitro pharmacological characterization of novel isoxazolopyridone derivatives as allosteric metabotropic glutamate receptor 7 antagonists. *J Pharmacol Exp Ther* **323:**147–156.

Urban JD, Clarke WP, von Zastrow M, Nichols DE, Kobilka B, Weinstein H, Javitch JA, Roth BL, Christopoulos A, Sexton PM, et al. (2007) Functional selectivity and classical concepts of quantitative pharmacology. *J Pharmacol Exp Ther* **320:**1–13.

Wu S, Wright RA, Rockey PK, Burgett SG, Arnold JS, Rosteck PR Jr, Johnson BG, Schoepp DD, and Belagaje RM (1998) Group III human metabotropic glutamate receptors 4, 7 and 8: molecular cloning, functional expression, and comparison of pharmacological properties in RGT cells. *Brain Res Mol Brain Res* **53:**88–97.

Zhang Y, Rodriguez AL, and Conn PJ (2005) Allosteric potentiators of metabotropic glutamate receptor subtype 5 have differential effects on different signaling pathways in cortical astrocytes. *J Pharmacol Exp Ther* **315:**1212–1219.

Address correspondence to: Dr. Colleen M. Niswender, 1215 MRB IV, Department of Pharmacology, Vanderbilt University, Nashville, TN 37232. E-mail: colleen.niswender@vanderbilt.edu